Two Approaches for Dense DSM Generation from Aerial Digital Oblique Camera System

Massimiliano Pepe and Giuseppina Prezioso

Department of Sciences and Technologies, University of Naples "Parthenope", Centro Direzionale Isola C4, Naples, Italy

Keywords: Oblique Camera System, DSM, Photogrammetry, GPU, SfM, Aerial Survey.

Abstract: In recent years, in photogrammetric field, have been developed technologies, which consist of multi digital oblique camera, able not only to observe the same target from different angles, but also to determine, thanks to appropriate dedicated software, the geometry. Of particular interest is the new oblique camera system Leica RCD30 that combines vertical (nadir) and oblique cameras according to the "Maltese cross" characteristic scheme. The purpose of this work is to verify the potential of the oblique imagery to provide dense point clouds to realize Digital Surface Model (DSM) to high resolution, where for high-resolution model is meant a representation of the observed scene with a ground sample distance (GSD) of less than 10cm. The dense Digital Surface Models are obtained through two different approaches, one that derived from photogrammetric reconstruction based on graphic processing units (GPU) technique and multi-core CPUs, the other from so-called Structure from Motion (SfM). To analyse the quality both of acquisition systems that the model surface obtained from images, a case study on the Nöllen (Switzerland) area is presented.

1 INTRODUCTION

The oblique camera system is designed for high accuracy 3D city models (Zhang et al., 2004, Wang et al., 2008), cadastral applications (Pepe et al., 2012), cultural heritage field (Nocerino et al., 2013) and for the realization of DSM (Le Besnerais, 2008; Madani, 2012; Cavegn, 2014).

Especially for the production of DSM, the recent development of dense image matching methods, by deriving point clouds from imagery, provides an efficient alternative at airborne LiDAR systems (Fritsch et al., 2012). In fact, the first experiments the 3D point clouds concerning by oblique camera have shown the potential using sample image processing algorithm and the very dense point clouds can be filtered to obtain even digital terrain models (Fritsch et al., 2013).

The actual oblique camera system comes in a variety of configurations, which differ in the sensors number, format, arrangement, mode of acquisition and spectral sensitivity (Rupnik et al., 2014).

The oblique camera system taken into consideration in this paper is the Leica RCD30 Oblique Penta System, which consists of five cameras: four cameras inclined at 35° and arranged according to an orientation north, south, west, east and one nadir camera.

The shape of the ground coverage captured simultaneously by the five cameras looks like a "Maltese Cross" (Figure 1), a term first coined by Gordon Petrie and Kenneth Smillie (Petrie, 2009). The several cameras are mounted rigidly together and their geometric configuration is calibrated to enable accurate measurements in both the vertical and oblique images.
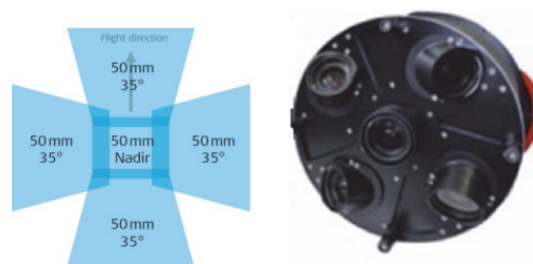
Figure 1: Leica RCD30 Oblique Penta footprint with RCD30 cameras.

The Leica RCD30 medium format camera is the first 60 Mp camera able to acquire co-registrated multispectral RGB and NIR imagery from one

camera head (Wagner R., 2011). The features of camera are reported in Table 1 (Leica Geosystems, 2015).

Table 1: Features of Leica RCD30 Oblique Penta.

CCD Size	8956 x 6708 *pixels*
Pixel Size	6 *µm*
Dynamic Range of CCD	73 *dB*
Resolution A/D Converter	14 *bit*
Maximum Frame Rate	(Penta) 1.8 *sec*
Motion Compensation	Mechanical, bi-directional
Spectral Range	Coregistered

Furthermore, this sensor connected with GNSS/INS systems allows to accelerate the workflow for the construction of elevation models. In fact, the direct georeferencing (DG) system correlates directly the data collected by a remote sensing system to the Earth, by accurately measuring the geographic position and orientation of the sensor without the use of the traditional ground-based measurements (Mostafa et al., 2001; Cramer, 2010; Pepe et al., 2015a).

In addition to the acquisition system is necessary define the appropriate processing technique of image. The following section describes two approaches.

The first coming from the computer vision community and known as Structure From Motion (SfM) algorithms while the second approach is based on use of the GPU technology in combination with multi-core CPUs which produces unmatched processing speeds for the creation of geospatial data. In the two approaches the quality of the DSM depends by image of the photogram or better, within the period of digital photogrammetry, by the Ground Sampling Distance (GSD).

2 GSD, SCALE NUMBER AND ACCURACY OF THE OBLIQUE IMAGES

For each digital camera, the combination of the focal length and pixel size determines a specific Ground Sampling Distance (GSD).

In the case of vertical aerial flight, the relationship between the GSD to the relative flight altitude is (Neumann, 2008):

$$GSD = \frac{H}{f}S \qquad (1)$$

where:

GSD	Ground Sampling Distance;
f	Focal length;
S	Pixel size;
H	Relative flight altitude.

Considering the Leica RCD30 camera, using a focal length of 50 mm and a pixel size of 6 µm, the relation between the flight altitude and the GSD, in the case of vertical aerial flight, is reported in Table 2.

Table 2: GSD at different flight altitude in vertical aerial survey.

GSD (cm)	Image scale	Height above ground (m)	Footprint along track (m)	Footprint cross track (m)
3	1:5000	250	20125	26870
5	1:8333	417	33542	44783
8	1:13333	667	53667	71653
10	1:16667	833	67083	89657
15	1:25000	1250	100625	134350
20	1:33333	1667	134167	179133
30	1:50000	2500	201250	268700
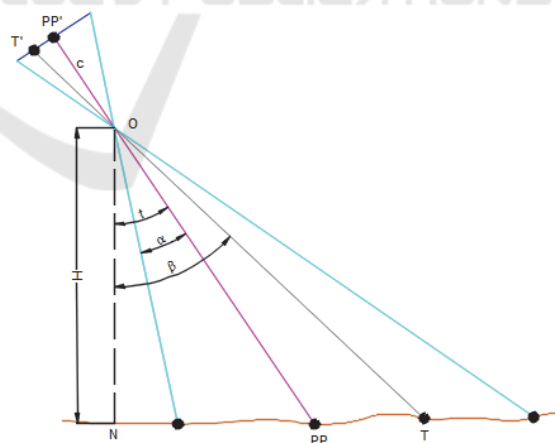
Figure 2: Parameters of oblique images (Hohle, 2008).

The scale within an oblique image (Figure 2) depends of several parameters (Hohle, 2008), as shown below:

$$m = \frac{H \cos (\beta - t)}{f \cos \beta} \qquad (2)$$

where:

m	Scale at target point;
t	Tilt angle;
β	Angle between the viewing ray to a target and the vertical;
α	Half of field of view.

The scale, $m_{PP'}$, at principal point of image, PP', is:

$$m_{PP'} = \frac{H}{f \cos t} \tag{3}$$

By fixing the flight altitude (derived from Table 2 for each GSD) and choosing the parameters of the photogrammetric system under consideration, the scale at principal point of an image oblique assumes the values given in Table 3.

Table 3: Scale at the principal point using the RCD30 system parameters.

Relative flight altitude (m)	Image scale	GSD (cm)
250	1:6104	4
417	1:10181	6
667	1:16285	10
833	1:20338	12
1250	1:30519	18
1667	1:40701	24
2500	1:61039	37

This means that at the same flight altitude occur several GSD according to the cameras scheme and, as can be observe from Tables 2 and 3, with increasing altitude, the difference in GSD between vertical and oblique aerial flight becomes more important.

For example considering the flight altitude of 2500 m, if the flight of acquisition is vertical we get a GSD = 30 cm, whereas if we choose the oblique aerial flight we get a GSD = 37 cm.

Therefore, the GSD varies depending on the geometry of the photogrammetric aerial oblique flight and this is to be taken into account in the planning phase of flight to obtain a specific accuracy.

In the study the accuracy of oblique stereo image occurs two cases: tilt across track (side-looking) and tilt along track (forward-looking), whose geometry in oblique stereo image is shown in figure 3 (Gerke, 2009).
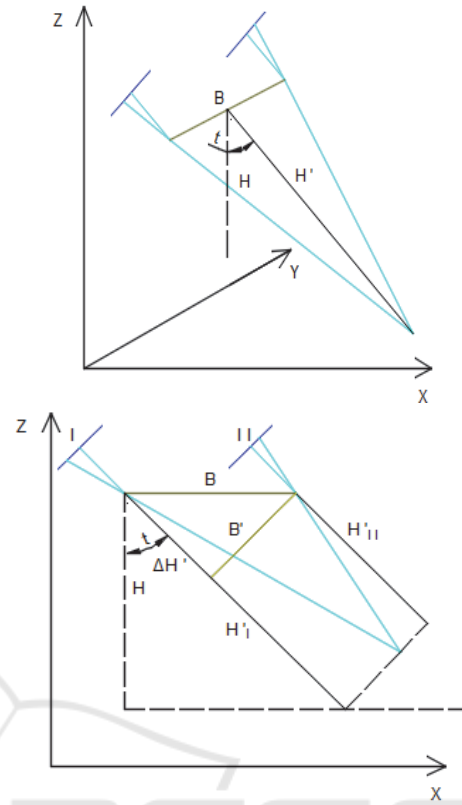
Figure 3: Several geometry in oblique stereo image – looking across track (up) and along track (down).

In the first case (tilt across track) the accuracy value (Gerke, 2009) is:

$$\begin{cases} \sigma_H \cong \sqrt{(\sigma_H' \cos t)^2 + (\sigma_{X,Y}' \sin t)^2} \\ \sigma_{X,Y} \cong \sqrt{(\sigma_H' \sin t)^2 + (\sigma_{X,Y}' \cos t)^2} \end{cases} \tag{4}$$

where:

$$\sigma_H' \cong \frac{H'}{B} m \, \sigma_{p_x} \tag{5}$$

$$\sigma_{X,Y}' \cong \frac{1}{2} m \, \sigma_{p_x} \tag{6}$$

and indicating with:

σ_{p_x}' parallax accuracy

$$H' = mf \tag{7}$$

In the second case (tilt along track) the accuracy (Gerke, 2009) is:

$$\begin{cases} \sigma_{H_I'} \cong \sigma_{H_{II}'} \cong \sqrt{\left(\frac{H_{II}'}{p_x}\right)^2 \sigma_{p_x}^2 + \left(\frac{B' \sin t}{p_x}\right)^2 \sigma_{p_x}^2} \\ \sigma_{X,Y}' \cong \frac{H_I'}{f} \sigma_x \end{cases} \tag{8}$$

where:

p_x parallax which needs to be computed for the estimation.

$$B' \cong B \cos t \qquad (9)$$

$$\Delta H' \cong B \sin t \qquad (10)$$

$$H'_I \cong m f \qquad (11)$$

$$H'_{II} \cong H'_I - \Delta H' \qquad (12)$$

3 CASE STUDY

The nadir and oblique images are in Tiff format and have been acquired on the Nöllen area, Widnau, Switzerland (Figure 4).

The complete block consists of 625 images at 5 cm GSD and 300 images at 8 cm GSD with 30% side overlap and 60% forward overlap. The external orientation of every image captured, given in UTM Zone 32 North, is calculated using the software IPASCO and the Leica Photogrammetry Suite. The misalignments and principal points of auto-collimation (PPA), for the five different cameras, have not been corrected in this original dataset. Of this photogrammetric block has been selected a limited area of particular interest and were chosen the frames of the flight plan with GSD equal to 5cm.
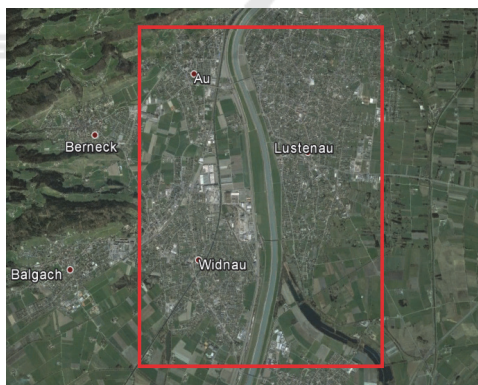
Figure 4: A snapshot from Google Earth® showing the location of the study area.

The file size of each aerial photo is about 487 MB. The processing was carried out using a PC with the following configuration: Intel® Core™ 2.50 GHz CPU, 8 GB RAM.

3.1 DSM by using Structure from Motion (SfM) Photogrammetry

Many tools designed for SfM applications collapse due to the enormous number and size of the images used in mapping projects. An idea to overcome this limitation is to exctract from the block a photogrammetric sub-block. In particular, have been used 12 pictures of the block having a GSD of 5 cm in order to obtain a higher resolution of the DSM and orthophoto. The images have been chosen to allow a stereoscopic coverage both in the sense of the flight that transversely.

In this section, Agisoft Photoscan Pro software (Agisoft, 2014) was used for 3D data processing. This software works mainly on computer vision based techniques. Structure from Motion (SfM), and multi-view reconstruction techniques are the main principles on which Agisoft creates the 3D model of an object. In this software, both image alignment and 3D model reconstruction are fully automated (Sing, 2014). The 3D model reconstruction is obtained in several straightforward processing steps.

Firstly Agisoft allows, through an algorithm called "*feature detection algorithm*" by identify, automatically, features in overlapping pictures and match them. When the process is repeated for all feature points in the dataset, the result is a sparse point cloud which is a 3D approximation of the scene in the pictures (Semyonov, 2011). The alignment operation of the 12 images was performed in 435 seconds. At this point, since both the original camera positions and the cameras calibration are known, the software can build a dense points cloud (Van Damme, 2015) using a more computationally-intensive algorithm. The Agisoft software offers different options for to construct the dense points clouds (Low, Medium, High, Very High), among them the authors have chosen the "High", because the computer was not able to process in "Very High" mode.

Subsequently, in the "*Build Mesh*" step, PhotoScan creates a surface mesh from the dense point cloud. A representation of the geometry of the images and the DSM generated in Agisoft environment, is shown in Figure 5.

The software enable the export the point clouds in several format; the LAS ASPRS file format allows quickly to read and interpret the elevation ASCII data and at the same time reduces the file size. However, GNSS systems have led to the use of the ellipsoidal height and, consequently, also the point clouds are obtained in the ellipsoidal reference system. To transform the ellipsoidal in ortometric height is necessary to know a geoid undulation model. The geoid undulations was taken from the geoid model EGM2008 (Pavlis et al., 2008) and, with using a software developed in Matlab® by the authors, has been possible to transform the point clouds from

ellipsoidal to orthometric height (Pepe et al., 2015b).
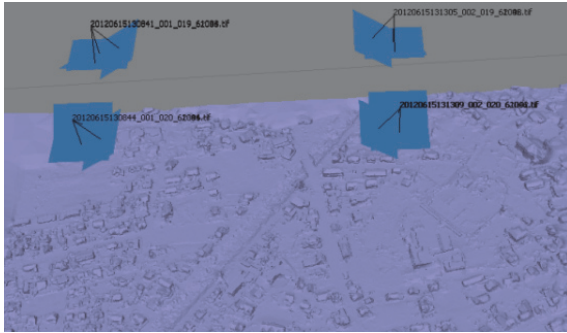
Figure 5: Camera positions and elevation model.

Subsequently the point clouds obtained were converted into raster format GeoTiff with grid 10cmx10cm (Figure 6).
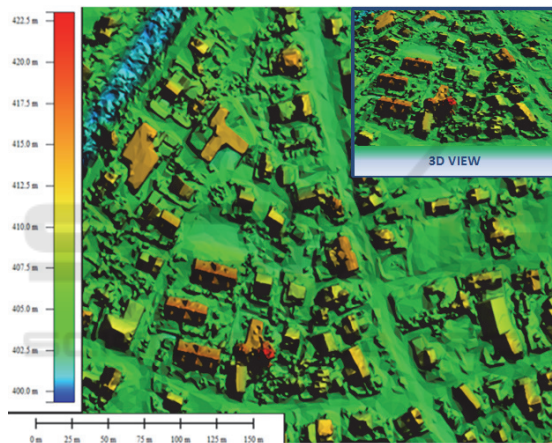
Figure 6: DSM of the study area obtained with Agisoft Photoscan Pro.

3.2 DSM Obtained using GPU Method

In recent years is becoming more common, in photogrammetric applications, the use of parallel programming and computing power of the graphics processing unit. In fact the modern graphic processing units are not only powerful graphic engines but also they are high level parallel programmable processors with very fast computing capabilities and high-memory bandwidth speed compared to central processing units (CPU) (Sahin, 2012).

A commercial software that uses this approach is Correlator3D ™ with which it is possible to realize a DSM in two main phases: the aerial triangulation and, subsequently, the generation of the model.

The first task for the production of the DSM is the "*Aerial triangulation*", which begins with the extraction of the tie points. Correlator3D™ calculates the tie points by identifying, in adjacent images, some feature points common and once done that, these feature points are matched within each flight line between adjacent images. The final step in aerial triangulation is the "*Bundle adjustment*". In this process is performed, on all the images, a minimization routine which determines, in iterative mode, a unique correction for the exterior orientation (EO) parameters in such a way as to reduce the average residual between the tie points and the projected points (Simactive, 2015). For DSM generation is used the graphics processing unit where the images are loaded into the GPU the memory on a pair-by-pair basis, significantly reducing the memory constraints on the system. The process begins by loading a pair of images into the GPU memory and a DSM patch, corresponding to such pair, is created and stored on disk. This process repeats until all the images have been processed. The resulting overlapping DSM patches are then optimized and merged in the following manner. Within every DSM patch, to each point is associated a weight based on a confidence measure. This measure depends on different metrics including one that assigns a weight to the elevation values as a function of their distance from the center of the DSM patches, this to reduce the potential occlusion problems (Rotenberg, 2013). In the phase of the Aerial Triangulation the average tie point residual error was of 0.36 pixel and the required processing time for obtain the DSM has been of some minutes.
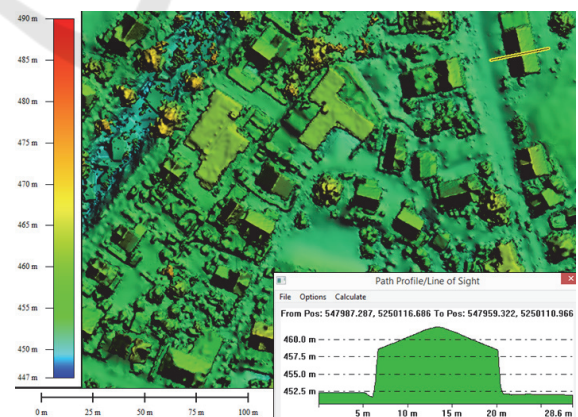
Figure 7: DSM of the study area, by Correlator3D™ software, and profile elevation (ellipsoidal height).

The DSM realized by Correlator3D™, and represented in Global Mapper environment (Figure 7), shows the quality with which the software can

describe the territory. In fact, from the elevation profile it can be seen not only the typical shape of the roofs and of the shape of the buildings, but also the shape of the street gutter. Subsequently, in order to check if the software shows limitations in the treatment of numerous images, has been analysed a block photogrammetric much wider of that previously used. From this test it was found that the software has been able to process 625 images, in 4725 sec. for the aerial triangulation processing and 81000 seconds for the production of the DSM.

3.3 DSM Comparison

The two DSM were compared with each other both in terms of quantity and quality. From the quantitative point of view means to compare the two models both planimetrically that altimetrically. The results obtained using some of the benchmark showed a shift planimetric and altimetric contained in the order of a few centimetres. The qualitative comparison aims to analyse the ability, of the DSM, to represent spatial objects (houses, dormers, trees, etc.). The DSM, which has been produced, with Correlator3D™ has allowed a (little) better description of spatial objects than to Agisoft software (Figure 8).
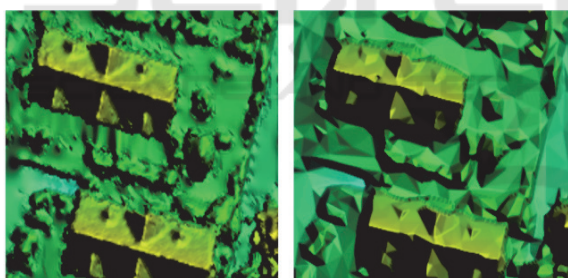
Figure 8: DSM comparison - Correlator3D™ (left) and Agisoft (right).

Nevertheless qualitative and quantitative aspects are interrelated. For example if the model obtained with Agisoft is not able to represent a tree or a fence means that this DSM, compared with that generated by Correlator3D™, will get of the height differences also important. In order to quantify the difference between the two DSM, obtained with different approachs, it has been employed the QuantumGIS software, using the mathematical operator raster "*difference*".

From the comparison of the raster maps (Figure 9) can be deducted the following considerations:

✓ the vast majority of the territory has a difference contained in the value of 5 cm, demonstrating the

accuracy that can be achieved with both software tested;

✓ the only elements that showing notable differences in height are the trees;

✓ few and limited vertical shift occurred along the edges of some buildings with the ability to Correlator3D™ to produce a point cloud denser and therefore represent in greater detail some spatial objects; this means that a more dense point clouds allows you to distinguish some structures of the building, such as gutters, chimneys and protruding elements.
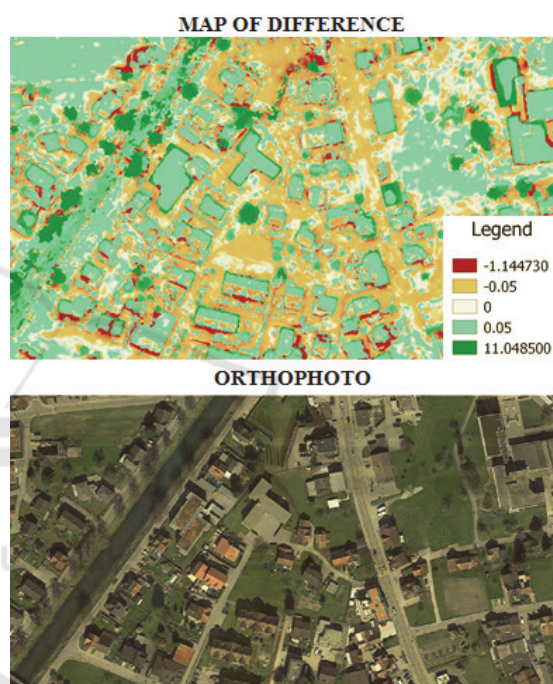
Figure 9: Difference Map (meters) between the two models (up) and orthophoto (down).

As regards processing times, the point clouds generated by the software Correlator3D™ are obtained in a time less than Agisoft. In addition the first software showed a greater capacity to handle a large number of images and, consequently, to represent a wider area of the territory.

4 CONSIDERATION ON AERIAL SURVEYS WITH OBLIQUE CAMERAS SYSTEM

The traditional photogrammetric workflow overlap (60% forward and 30% side overlap) creates occlusion areas and reduces the redundancy of

image information. Therefore it is desirable in the flights on the cities, to increases the overlap of the images, regardless of the type of restitution.

The high overlap allows a higher probability of successful matches but, at the same time, a small base line involves in a low accuracy of the height, as shown in the formula 4 and 8. This means that, wanting to ensure a thorough and detailed DSM, the flight plan has to be well designed.

Also it is necessary to make an observation of an operational character: the high spatial resolution of the images requires a low-level flight. The low altitude atmospheric air is influenced by topography and the local temperature field. This means that a rotation of the aircraft can affect not only the quality of photogrammetry, but also cause the observation of elements not belonging to scene, that is, in other words, can happen of to photograph the underside of the aircraft or the aircraft hatch (Figure 10). All this results in saying that the flight preparation requires appropriate meteorological conditions and a proper study of the flight planning.

Figure 10: Elements of the aircraft visible in the photo.

5 CONCLUSIONS

Through the use of image from digital oblique camera system, the two software examined have provided, in an automatic way, dense point clouds and of high accuracy, of particular utility in many fields of geomatics.

The approach SfM for the production of DSM using aerial digital image of medium format is possible, but unfortunately limited to a few images.

The division into sub-blocks of the entire aerial survey has allowed to overcome, at least in part, this problematic. However, the processing time becomes too long if the work area is very extensive. Instead,

the dense Digital Surface Models obtained through photogrammetry reconstruction based on GPU technology and multi-core CPUs has allowed to obtain not only accurate point clouds but enabled to manage a block photogrammetric with a lot of images.

REFERENCES

Agisoft LLC, 2014. Agisoft PhotoScan User Manual: Professional Edition, Version 1.1. http://www. agisoft.ru/products/photoscan. Accessed 20/01/2015

Cavegn, S., Haala, N., Nebiker, S., Rothermel, M., Tutzauer, P., 2014. Benchmarking high density image matching for oblique airborne imagery, *The International Archives of the Photogrammetry, Remote Sensing and Spatial Information Sciences, Volume XL-3*, 5 – 7 September 2014, Zurich, Switzerland.

Cramer, M., 2010. Direct georeferencing using GPS/INERTIAL exterior orientations for photogrammetric applications. *International Archives of Photogrammetry and Remote Sensing*, Amsterdam, Holland, 33, pp. 198 –205.

Fritsch, D., Kremer, J., Grimm, A., 2012. Towards All-in-one Photogrammetry. *GIM International*, Vol. 26(4), pp. 18-23.

Fritsch, D., and Rothermel, M., 2013. Oblique image data processing: potential, experiences and recommendations. *Proc. 54th Photogrammetric Week*, pp. 73 – 88.

Gerke, M., 2009. Dense matching in high resolution oblique airborne images. In: *CMRT09: Object extraction for 3D city models, road databases and traffic monitoring: concepts, algorithms and evaluation*, Paris, 3–4 September 2009, pp. 77 – 82.

Höhle, J., 2008. Photogrammetric measurements in oblique aerial images. *Photogrammetrie Fernerkundung Geoinformation 1*, pp. 7 – 14.

Rotenberg, K., Simard, L., Simard, P., 2013. Dense DSM Generation Using the GPU*, Photogrammetric Week 2013*, pp. 285 – 295.

Le Besnerais, G., Sanfourche, M., Champagnat, F., 2008. Dense height map estimation from oblique aerial image sequences. *Computer vision and image understanding*, 109(2), pp. 204-225.

Leica Geosystems, 2015. http://www.leica-geo systems.com. Accessed 01/03/2015

Madani, M., 2012. Accuracy potential and applications of Midas aerial oblique camera system, *International Archives of the Photogrammetry, Remote Sensing and Spatial Information Sciences*, Volume XXXIX-B1, Melbourne, Australia.

Mostafa, M. R., Hutton, J., Lithopoulos, E., 2001. Airborne direct georeferencing of frame imagery: an error budget, *The 3ʳᵈ International symposium on mobile mapping technology*, Cairo, Egypt.

Neumann, K. J., Trends for digital aerial mapping cameras, *The International Archives of the Photogrammetry, Remote Sensing and Spatial Information Sciences*, 2008.– Vol.XXXVII.– Part B1, pp. 551 – 554.

Nocerino, E., Menna, F., Remondino, F., Saleri, R., 2013. Accuracy and block deformation analysis in automatic UAV and terrestrial photogrammetry – Lesson learnt. *ISPRS Annals of the Photogrammetry, Remote Sensing and Spatial Information Sciences*, Vol. II (5/W1), pp. 203 – 208.

Pavlis, N., K., Holmes, S., A., Kenyon, S., C., Factor, J., K., 2008. An Earth Gravitational Model to Degree 2160. EGM2008, *General Assembly of the EGU*, Vienna, April 13 – 18/2008.

Pepe, M., Prezioso, G., Santamaria, R., 2012. Calcolo della rendita presunta degli immobili fantasma: contributo delle immagini aerofotogrammetriche da multicamere digitali oblique. *Atti 16a Conferenza Nazionale ASITA*, 6 – 9 novembre 2012, Fiera di Vicenza, pp. 1091 – 1095.

Pepe, M., Prezioso, G., Santamaria, R., 2015a. Impact of vertical deflection on direct georeferencing of airborne images. *Survey Review*, Vol. 47, Issue 340, pp. 71 – 76.

Pepe, M., Prezioso, G., 2015b. A Matlab geodetic software for processing airborne LIDAR bathymetry data, *ISPRS - International Archives of the Photogrammetry, Remote Sensing and Spatial Information Sciences*, Volume XL-5/W5, 2015, pp. 167 – 170.

Petrie, G., 2009. Systematic oblique aerial photography using multiple digital frame cameras. *Photogrammetric Engineering & Remote Sensing*, Vol. 75, No. 2, pp. 102 – 107.

Rupnik, E., Nex, F., Remondino, F., 2014. Oblique multi-camera systems – Orientation and dense matching issues, *International Archives of the Photogrammetry, Remote Sensing and Spatial Information Sciences*, Volume XL-3/W1, pp. 107 – 114.

Sahin, H., S., Kulur, 2012. Orthorectification by using GPU method. *International Archives of the Photogrammetry, Remote Sensing and Spatial Information Sciences* 39, 165 – 170.

Semyonov, D., 2011. Algorithms used in PhotoScan. *Agisoft Community Forum*. www.agisoft.com/forum/index.php?topic=89.0. Accessed 6/08/2015

Simactive, 2015. http://www.simactive.com/en/software-description Accessed 8/8/2015

Singh, S. P., Jain, K., Mandla, V.R., 2014. A new approach towards image based virtual 3D city

modeling by using close range photogrammetry, *ISPRS Ann. Photogramm. Remote Sens. Spatial Inf. Sci., II-5,* pp. 329–337.

Van Damme, T., 2015, Computer vision photogrammetry for underwater archaeological site recording in a low-visibility environment, *Int. Arch. Photogramm. Remote Sens. Spatial Inf. Sci., XL-5/W5*, pp. 231 – 238.

Wagner R., 2011. The Leica RCD30 Medium Format Camera: Imaging Revolution, *Photogrammetric week*. Stuttgart, Germany, pp. 89 – 95.

Wang, Y., Steve, S., Frank, G., 2008, Pictometry's proprietary airborne digital imaging system and its application in 3D city modelling. *International Archives of Photogrammetry, Remote Sensing and Spatial Information Sciences* 37, pp. 1065 – 1069.

Zhang, Z., Wu, J., Zhang, Y., Zhang, Y., Zhang, J., 2004. Multi-View 3D City Model Generation with Image Sequences. *International Archives of Photogrammetry and Remote Sensing*, Istanbul, Turkey, Vol. 34, Part 5, pp. 351-356.